Improvement of the Effective Mass Approximation for Silicon Nanowires

Aniello Esposito[1], **Martin Frey**[1] **and Andreas Schenk**[1]

[1] Integrated Systems Laboratory, ETH Zurich, Gloriastrasse 35, CH-8092, Switzerland

esposito@iis.ee.ethz.ch

Introduction

SEMICONDUCTOR nanowires (NW) are assumed to play an important role in the future of nanoelectronics as they can act both as active devices (transistors) and as wire connectors. Several materials such as Si, GaAs, and Ge can be used for building NWs with different cross sectional shapes and channel orientations. Computer simulations of NWs help to gain deeper physical insights and support the experimental development techniques in conjunction with the fabrication of such novel devices. In the regime of a few tenths of nanometers the quantum mechanical treatment, i.e.the solution of the Schrödinger equation, becomes inevitable. A possible way to include the atomistic character of NWs is given by the pseudopotential [3] method. Further simplifications lead to the more manageable empirical pseudopotential methods (EPM) [4] which have been extensively investigated in the case of silicon [5]. The effective mass approximation finally represents the most popular approach used in present device simulators [1].

The first part of this work is concerned with the application of the EPM to silicon nanowires as well as the introduction of the EMA. The discrepancy between the EMA and EPM are discussed in the case of a weak harmonic potential and a simple improvement of the EMA is presented in the end.

Theory

IN this work the NWs are assumed to be carved out of a bulk crystal without any a posteriori relaxation treatment. The single-particle Schrödinger equation describing an electron in an arbitrary crystal is given by

$$\left[-\frac{\hbar^2}{2m_e}\Delta + V(\vec{r})\right]\Psi(\vec{r}) = E\Psi(\vec{r}), \tag{1}$$

where m_e is the electron mass and $V(\vec{r})$ is periodic with respect to a unit cell Ω spanned by three vectors $\{\vec{a_1}, \vec{a_2}, \vec{a_3}\}$. Blochs theorem states that the solution of Eq. (1) has the form

$$\begin{aligned}\Psi(\vec{r}) \;&\rightarrow\; \Psi_{n,\vec{k}}(\vec{r}) = \exp(i\vec{k}\vec{r})u_{n,\vec{k}}(\vec{r})\\ E \;&\rightarrow\; E_n(\vec{k}),\end{aligned} \tag{2}$$

where $n \in \mathbb{N}$ and $E_n(\vec{k})$ is referred to as the *bandstructure*. The vector $\vec{k}$ belonging to the so called *reciprocal* space is restricted to $\widehat{\Omega} \equiv \mathrm{span}\{\vec{b_1}, \vec{b_2}, \vec{b_3}\}$, where $\vec{b_i}$ are given as the columns of the matrix $2\pi(\vec{a_1}, \vec{a_2}, \vec{a_3})^{-1}$ for $i = 1, 2, 3$. Furthermore, the function $u_{\vec{k}}(\vec{r})$ from Eq. (2) is periodic w.r.t. the unit cell Ω and can be expressed in terms of plane waves

$$u_{n,\vec{k}}(\vec{r}) = \sum_{\vec{G}\in\Lambda} c(\vec{G})\exp(i\vec{G}\vec{r}), \tag{3}$$

where $\Lambda = \{n_1\vec{b_1} + n_2\vec{b_2} + n_3\vec{b_3} \mid n_1, n_2, n_3 \in \mathbb{Z}\}$. For computational purposes the set Λ from Eq. (3) is reduced to $\widetilde{\Lambda} \equiv \{\vec{G} \in \Lambda \mid \hbar^2\vec{G}^2/(2m_e) \leq C\}$ for a given cutoff energy C. In order to obtain an equation for $u_{n,\vec{k}}(\vec{r})$ the ansatz from Eq. (2) is used in Eq. (1) yielding the secular equation

$$\left[\frac{\hbar^2}{2m_e}\left(-i\vec{\nabla} + \vec{k}\right)^2 + V(\vec{r})\right]u_{n,\vec{k}}(\vec{r}) = E_n(\vec{k})u_{n,\vec{k}}(\vec{r}). \tag{4}$$

For a given vector $\vec{k}$ the secular problem given in Eq. (4) is solved on the unit cell Ω yielding a discrete set of eigenvalues parametrized by n which finally compose the bandstructure $E_n(\vec{k})$. The EMP employs a superposition of atomic pseudopotentials $V_{\mathrm{atom}}(|\vec{r}|)$, i.e.

$$V(\vec{r}) = \sum_{\vec{R}_{\mathrm{atom}}} V_{\mathrm{atom}}(|\vec{r} - \vec{R}_{\mathrm{atom}}|), \tag{5}$$

in order to approximate the screened potential $V(\vec{r})$ from Eq. (1). The effective potential $V_{\mathrm{atom}}(|\vec{r}|)$ given in Eq. (5) is adjusted to fit either experimental or *ab-initio* calculated data. In Ref. [5] the V_{atom} are fitted to the bulk Si bandstructure, effective masses, and the surface work function.

Nanowire Bandstructure

THE unit cell containing the wires portion from which the entire nanostructure is generated via periodic continuation is given by $\Omega = [0, L_x] \times [0, L_y] \times [0, L_z]$. While $L_x = a = 0.543$ nm the L_y and L_z delimit the transverse wire extensions including the hydrogen passivated surface as well a vacuum layer. The wires interior mainly consists of silicon blocks of size $a \times a \times a$ which are transversally aligned. A plot of a nanowire consisting of 4×4 blocks is given in Fig. 1. In the following the wires are assumed to have a square cross section and the width is specified by a number of blocks. The wire bandstructure can be computed according to Eq. (1) and a plot of the bandstructure belonging to the 4×4 nanowire described in Fig. (1) is plotted in Fig. (2). Note the presence of an energy gap similar to the bulk case. The minumum of the upper energy portion is referred to as the lowest unoccupied molecular orbital (LUMO) and its probability density $|\Psi_{n,\vec{k}}(\vec{r})|^2$ is plotted in Fig. (3).

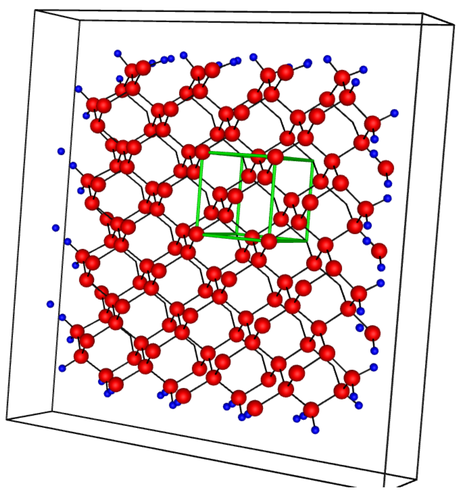

Figure 1: *The wire unit cell consisting of 4×4 blocks. A block is highlighted by the green box. Hydrogen and silicon atoms are denoted by the blue and red spheres respectively. The black box finally delimits the vacuum layer.*

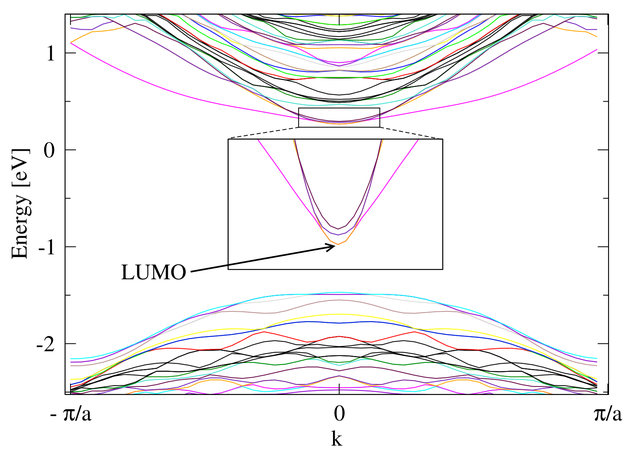

Figure 2: *The wire bandstructure plotted from $(-\pi/a, 0, 0)$ to $(\pi/a, 0, 0)$ according to the parametrization of Ref. [5]. The minimum of the upper energy portion is referred to as the lowest unoccupied molecular orbital (LUMO).*

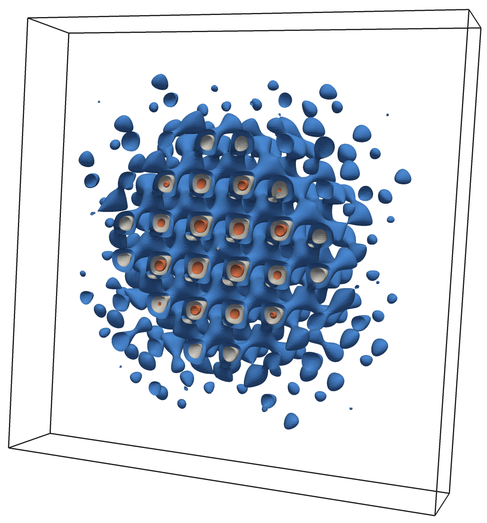

Figure 3: *The probability density of the lowest unoccupied molecular orbital. The bounding box is identical to the one shown in Fig. (1).*

EMA compared to the EPM

THE effective mass approximation considerably simplifies the expression given in Eq. (1) by dropping the potential term $V(\vec{r})$ at the cost of a slightly modified kinetic operator, i.e.

$$-\frac{\hbar^2}{2m_e}\vec{\nabla}^T\mathbf{M}\vec{\nabla}F(\vec{r}) = EF(\vec{r}), \tag{6}$$

where $F(\vec{r})$ is an approximation to the envelope of $\Psi(\vec{r})$ and $\mathbf{M}$ is parametrized according to Ref. [5]. Following Ref. [6] the case of a nanowire is mimicked by imposing Dirichlet boundary conditions to Eq. (6) according to the wires width. The LUMO energies computed via the EMA are compared to the EPM results for a set of wires and summarized in Fig. (4). The overestimation of the EPM energies by the EMA is a consequence of the confinement.

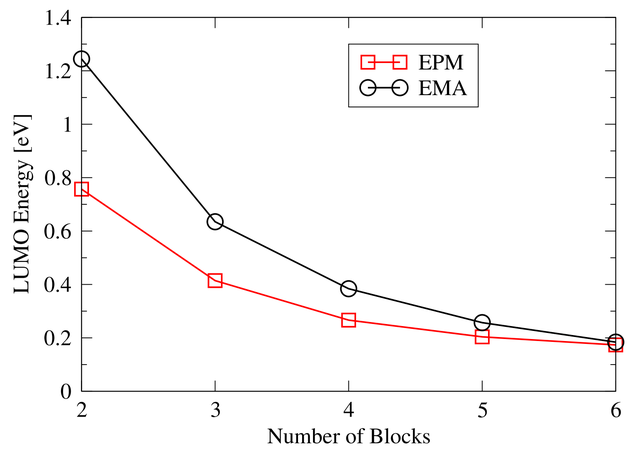

Figure 4: *The LUMO energies computed via the EMA are compared to the EPM results for different wire widths, i.e. number of blocks.*

Harmonic Perturbation

THE nanowire described in the previous section is now subjected to a weak harmonic perturbation of the form

$$U(\vec{r}) = \alpha(y^2 + z^2), \tag{7}$$

where α is width dependent and kept smaller than 0.05 $\mathrm{eV/nm^2}$. The resulting LUMO energies are lifted with respect to the free (unperturbed) case and summarized in Fig. (5). Again, the EMA is found to overestimate the EPM results. As the confinement is considered to be the major cause of this discrepancy compared to the harmonic perturbation a first step would be to reduce the EMA energies by the overestimation shown in Fig. (4), i.e. the free case. The shifted EMA energies are notably closer to the EPM results as can be seen in Fig. (5). Similar observations have already been made [6] while studying currents through silicon nanowires. The remaining difference between the shifted EMA and the EPM is roughly half as large as the effect caused by the harmonic perturbation and is related to the treatment of the boundaries as well as nonparabolicity or multi band effects which require more advanced approaches.

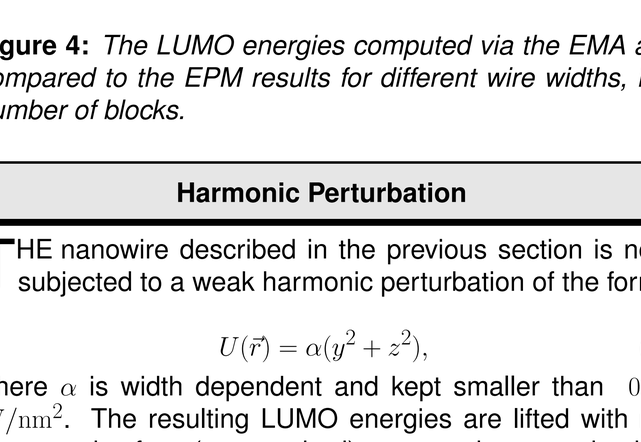

Figure 5: *The LUMO energies after adding a harmonic perturbation as described in Eq. (7). The circles denote the EMA results after shifting the values by the overestimation given in Fig. (4).*

The secular problem described in Eq. (4) is expressed in terms of plane waves as shown in Eq. (3). For the largest wires considered in this work the matrices reach sizes up to 9635×9635 and are solved by means of the ScaLAPACK.

Acknowledgements

THE authors are grateful for the financial support by the Swiss National Science Foundation (project NEQUATTRO SNF 200020-117613) and the European projects PULLNANO (IST-4-026828) and NANOSIL (IST-216171).

References

[1] F. O. Heinz and A. Schenk, J. Appl. Phys., no. 100 (2006), 084314.

[2] J. M. Luttinger and W. Kohn, Phys. Rev., no. 97 (1954), 869–883.

[3] W. E. Pickett Computer Physics Reports, no. 9 (1989), 115–198.

[4] M. L. Cohen and J. R. Chelikowsky, Springer Series in Solid-State Sciences 75.

[5] L. W. Wang and A. Zunger, J. Phys. Chem., no. 98 (1994), 2158–2165.

[6] J. Wang, A. Rahman, A. Gosh, G. Klimeck, and M. Lundstrom, IEEE Trans. on El. Dev., no. 52 (2005), 1589–1595.